UCRL-ID-125918

Detection of Leaks in Underground Storage Tanks Using Electrical Resistance Methods: 1996 Results

A. Ramirez
W. Daily

October 7, 1996

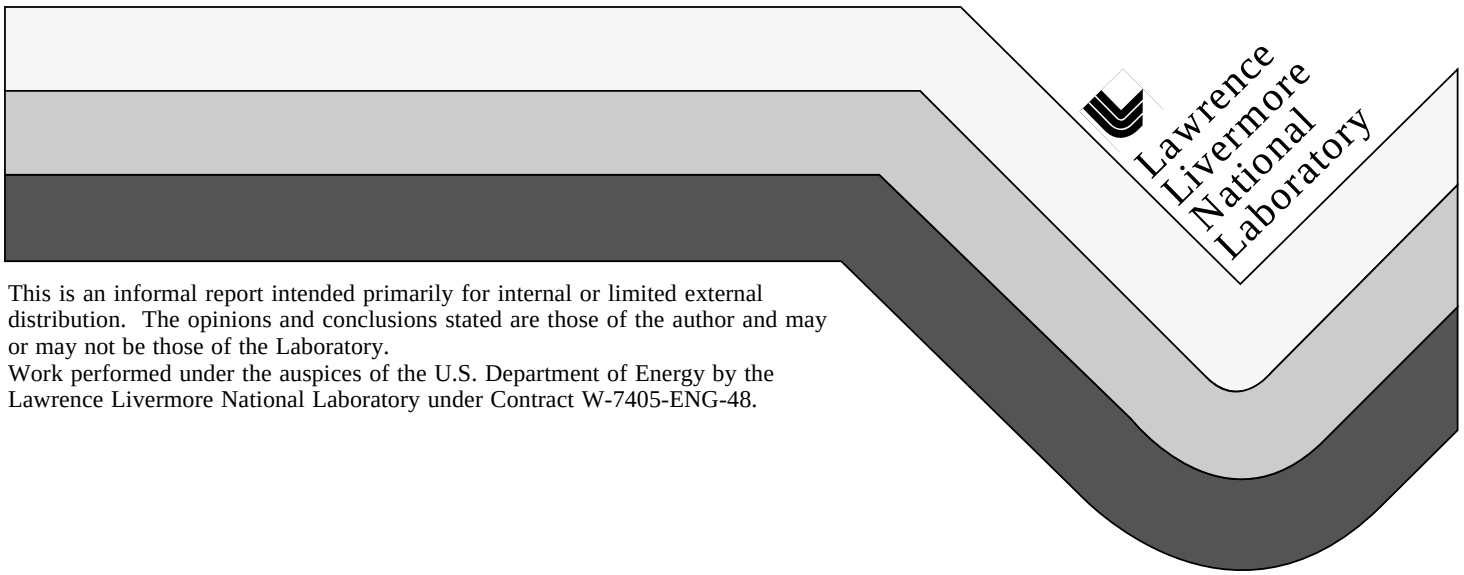

Work performed under the auspices of the U.S. Department of Energy by the Lawrence Livermore National Laboratory under Contract W-7405-ENG-48.

Detection of Leaks in Underground Storage Tanks Using Electrical Resistance Methods: 1996 Results

Abelardo Ramirez
William Daily

Lawrence Livermore National Laboratory
P.O Box 808, L-206
Livermore, CA 94550
off. 510-422-6909

Abstract:
This document provides a summary of a field experiment performed under a 15 m diameter steel tank mockup located at the Hanford Reservation, Washington. The purpose of this test was to image a contaminant plume as it develops in soil under a tank already contaminated by previous leakage and to determine whether contaminant plumes can be detected without the benefit of background data . Measurements of electrical resistance were made before and during a salt water release. These measurements were made in soil which contained the remnants of salt water plumes released during previous tests in 1994 and in 1995. The total volume of salt water released in 1994 and 1995 was about 10,750 liters. Thus, the test conducted in 1996 tested the sensitivity of electrical resistance measurements to a leak developing in the presence of previously established plumes. About 11150 liters of saline solution were released along a portion of the tank's edge in 1996. Changes in electrical resistivity due to release of salt water conducted in 1996 were determined in two ways: 1) changes relative to the 1996 pre-spill data, and 2) changes relative to data collected near the middle of the 1996 spill after the release flow rate was increased. In both cases, the observed resistivity changes show clearly defined anomalies caused by the salt water release. These results indicate that when a plume develops over an existing plume and in a geologic environment similar to the test site environment, the resulting resistivity changes are easily detectable. Three dimensional tomographs of the resistivity of the soil under the tank show that the salt water release caused a region of low soil resistivity which can be observed directly without the benefit of comparing the tomograph to tomographs or data collected before the spill started. This means that it may be possible to infer the presence of pre-existing plumes if there is other data showing that the regions of low resistivity are correlated with the presence of contaminated soil. However, this approach does not appear reliable in defining the total extent of the plume due to the confounding effect that natural heterogeneity has on our ability to define the margins of the anomaly.

1.0 Introduction:

In 1994 and 1995, field experiments were conducted under a 15 m diameter steel tank mockup located at the Hanford Reservation, Washington to evaluate the capabilities of Electrical Resistance Tomography (ERT) to detect leaks invading

the soil around metal tanks; the details of this work can be found in Ramirez et al, 1995. This work showed that ERT tomographs mapped the spatial and temporal evolution of resistivity changes caused by the leak; as the solution penetrated the soil, readily detectable resistivity decreases were observed and used to map the associated plume. The results showed that the metal tank has significant effects on the results obtained, primarily in reducing sensitivity to the leak.

The tests described here and in Ramirez et al., 1995, were designed specifically to address the issues of leaks from the single shell tanks built by the DOE during the cold war for storage of highly radioactive mixed wastes. The contents of these tanks is highly variable but typically the liquids are highly saline and therefore electrically conductive. Single shell and the double shell waste tank designs are common throughout the United States. The Department of Defense and industrial activities use thousands of storage tanks primarily for fuels, solvents, and other chemicals. The double shell tank design provides redundant containment barriers and allows detection of leakage prior to escape to the soil. The single shell tanks present potential environmental hazards because only a single barrier contains the liquids and any breach in the barrier will cause contaminant spillage. One method being considered to retrieve the waste is sluicing. This method will require recirculating thousands of gallons of water in the tank. If the sluicing method is used, it is possible to leak HLW into the soil. In other tanks, water is added to keep waste matrix from drying out and providing possible ignition to the flammable gases. For this reason a salt water tracer was used. For testing, an electrical equivalent (saline solution) was used instead of the real contaminant (radioactive nitrate solutions, see Cruse et al., for details) to preserve the environmental quality of the test site.

The presence of a metal tank with a resistivity of approximately 10^{-8} ohm-m embedded in soil with a resistivity of 10^{2} to 10^{3} ohm-m results in resistivity contrasts that are much larger than those found in natural geologic settings. One consequence of this large contrast is that a large fraction of the electrical current transmitted during a survey is shunted through the metal. This causes a significant reduction in the sensitivity of the measurements to the soil properties and in the ability to resolve the anomalies. Also, many of the assumptions made in formulating the forward and inverse problems are only valid for smaller contrasts.

The ERT method employed by Ramirez et al., (1995) was based on mapping the resistivity around and below a tank mockup. When the spillage of the liquids changes the electrical resistivity of the invaded soil in a measurable way, electrical resistivity tomographs can be used to map the resistivity changes caused by spillage. This strategy required that pre-spill measurements be available so that the pre-spill and post-spill resistivities could be compared. Such a strategy may be useful in operations such as tank sluicing were it is possible to collect pre-spill data prior to the start of a possible leak.

The ERT tests conducted at Hanford in 1994 and 1995 were conducted in soil that had not been previously disturbed by salt water plumes. In contrast, it is known that the soil around several tanks at the Hanford have released

radioactive salt solutions, thereby decreasing the soil resistivity relative to pristine conditions. This means that any future leakage due to activities such as sluicing will invade soil which has already been disturbed by previous leak(s).

The purpose of the test described here was to more closely represent the conditions which may exist around real tanks surrounded by contaminant plumes (Figure 1) and determine whether it is possible to: 1) use resistivity changes to map a contaminant plume as it developed in soil already contaminated by previous leakage, 2) image a contaminant plume when an active leak is present and current activities cause the leak flow rate to increase, and 3) detect leaks and map contaminant plume beneath a tank without the benefit of background (pre-spill) data .

1.1 Description of ERT:

Electrical resistance tomography (ERT) is a geophysical imaging technique which can be used to map subsurface liquids as flow occurs during natural or man-induced processes and to map geologic structure. Man-induced processes such as tank leaks and clean-up processes such as steam injection can create changes in a soil's electrical properties that are readily measured. Electrical resistance tomography is a technique for reconstruction of subsurface electrical resistivity. The result of such a reconstruction is a 2 or 3 dimensional map of the electrical resistivity distribution underground made from a series of voltage and current measurements from buried electrodes. The ERT approach we follow here relies on detection and mapping of the changes in electrical resistivity associated with a leak.

ERT surveys are performed using a number of electrodes in boreholes and/or at the ground surface to image the resistivity distribution between two boreholes. Using an automatic data collection and switching system, we collect a few hundred electrical resistance measurements. The data is then processed to produce electrical resistivity tomographs using state of the art data inversion algorithms. We use these measurements to calculate tomographs that show the spatial distribution of the subsurface resistivities.

1.2 Description of inverse algorithms:

Here we describe briefly some of the important features of the 2D and 3D algorithms. For additional details, the reader is referred to LaBrecque et al. (1996) (2D algorithm) and LaBrecque and Morelli (1996) (3D algorithm). Both algorithms involves solving both the forward and inverse problems. The forward problem is solved using a finite difference technique in the 3D problem and a finite element technique in 2D. Both algorithms implement a regularized solution which minimizes an objective function. The objective of the inverse routine is to minimize the misfit between the forward modeling data and the field data, and a stabilizing functional of the parameters. The stabilizing functional is the solution's roughness. This means that the inverse procedure tries to find the smoothest resistivity model which fits the field data to a prescribed tolerance.

1.3 Description of Experimental Site :

The following geologic description is based on geological information presented in a report by Reidel et al., (1992). The test site used for this work is part of the 200 East Area at the Hanford Site, located near Richland, Washington. The near surface sediments at the test site and throughout the Hanford Site were deposited during periods of Pleistocene cataclysmic flooding and Holocene eolian activity. The cataclysmic flooding occurred when ice dams in western Montana and northern Idaho were breached, allowing large volumes of water to spill across eastern and northern Idaho. The floods created a variety of deposits, including giant flood bars.

The test site is underlain by the Hanford formation, which includes one of the cataclysmic flood bars. The Hanford formation consists of pebble to boulder size gravel, fine to coarse grained sand, and silt. This formation is thickest in the vicinity of the 200 West and 200 East Areas where it is up to 65 m thick. The near surface sediments at the test site consist primarily of fine to coarse grained sand displaying plane lamination and bedding. Paleocurrent indicators within beds of plane laminated sands are unidirectional, generally toward the South and East. Hydraulic conductivities for these sediments depend upon the silt content, which is variable.

1.4 Description of the Field Test :

The field experiments were performed under a 15.2 m diameter steel tank mockup located at the Hanford Reservation (200 East Area). Figure 2 shows the layout at the leak detection experiment site. This empty steel tank contained several built-in spill points (three of which are shown). Sixteen boreholes with eight electrodes in each surrounded the tank. The electrodes were located in 10.7 m deep boreholes starting at the ground surface and spaced every 1.52 m. The diametrical distance between boreholes was 20.7 m.

This report covers the results obtained during a brine release experiment conducted from 5/29/96 to 6/10/96 at the leak test facility. About 11000 liters of saline solution were released along a portion of the tank's edge (side release point in Fig. 2) . The brine release was started at about 3:30 PM on 5/29/96 . The released volume is plotted as a function of time in Figure 3. The release rate varied from about 30 liters/hour to about 44 liters/hour depending on the ERT data being taken. The release rate is plotted as a function of time in Figure 4. Twenty-four kg of salt was added to every 3780 liters of Columbia River water and this resulted in an electrical conductivity of about 3 S/m (approximately that of sea water). Because this solution is lower salinity than the saturated brine in single shell tanks, it is a conservative tracer for this study. That is, if we can detect this tracer solution as a leak, then the brine from a tank will be easier to detect.

ERT data surveys were collected before, and during the brine release in each of 8 horizontal planes beneath the tank. The ERT measurements were made using a dipole-dipole approach. Plane 8 is a horizontal cross section at the ground surface 1.5 m above the bottom of the tank (so it contained the tank itself). Plane 7 is 1.5 m lower, a cross section level with the tank bottom. Plane 6 is 1.5 m below the tank bottom and so on to plane 1 which is 10.7 m below the ground

surface. This arrangement provided a series of 2D image planes at many levels which, when assembled together, gave an overall 3D view of the plume formed beneath the tank during the release and which could be used to determine the effects of imaging current shunted through the tank bottom.

To calculate the changes in the soil's electrical resistivity we compared a data set calculated for the case where a plume caused by a tank release is present, and a corresponding data set calculated for the case where there is no plume. One may consider performing the analysis by subtracting, pixel by pixel, images without the plume anomaly beneath the tank from those with the plume. However, this approach cannot be used because the two dimensional reconstruction algorithm will not converge using input data for which the boundary conditions are clearly three dimensional--the earth surface and the tank bottom are not accounted for in the forward model of the 2D code. Therefore, the comparison was performed by inverting the quantity

$$\frac{R_a}{R_b} \times R_h \qquad (1)$$

where R_a is the measured transfer resistance after the release, R_b is the transfer resistance before the release and R_h is the calculated transfer resistance for a model of uniform resistivity. The transfer resistance is simply the ratio of voltage to current for an individual 4 electrode measurement.

2.0 Results

2.1 Two dimensional resistivity change tomographs in the presence of a pre-existing plume:

In this section, we consider the scenario where a tank has leaked in the past but is not actively leaking when the first ERT surveys are made (Figure 1). This scenario assumes that a radioactive nitrate plume previously invaded some of the partially saturated soil surrounding the tank. With time, some of the salt water in the pore space drains away, leaving a region of increased moisture content and increased pore fluid conductivity. Then, a new leak springs from the tank (due to a sluicing operation) into the soil containing the remnant nitrate plume.

Figures 5 a and b present two-dimensional (2D) tomographs collected during the course of the salt water release. The released water penetrated soil already invaded by previous salt water plumes during the 1994 and 1995 tests. The location of the release point in 1996 releases is indicated on the figure. Each column of images shows the changes detected for a given time at various depths; the depth of images on each column increases from top (0 m. depth to bottom (10.7 m depth). Time and released volume increase from left to right on the figure. The images for June 30, 1996 at depths of 1.5, 3.0 and 4.6 m show clearly detectable electrical conductivity increases directly below the release point close to the "path for vertical migration". This behavior suggests that the brine is moving almost straight down as may be expected in reasonably homogeneous sandy soil present at the experimental site. Note that the changes observed increase in magnitude as time and spilled volume increase. Also, note that the bottom of the changing region deepens as time increases. The resistivity

decreases become larger over time (i.e. the resistivity ratios become increasingly different from 1.0, the condition of no change) implying that the flow paths are becoming more saturated with salt water. The position of the flow paths also appears to be stable over the period of the experiment.

The image at 4.6 m of depth seems to extend farther to the west than images above or below, thereby suggesting lateral spreading of the plume at this depth. This anomaly suggests that some of the released water has encountered a relatively less permeable layer at this depth which forces the water to travel sideways. Narbutovskih *et al.* (1996) have shown that a layer of caliche was observed at about 4.6 m depth in core samples from boreholes 40 to 50 ft to the East. It may be that the same caliche layer is responsible for the lateral fluid migration suggested by the images.

In 1994, a salt water release was conducted from the same release point used in the 1996 test. The 1994 results are shown in Figure 6 for comparison with the 1996 results shown in Figure 5. The 7/27/94 tomographs and the 5/31/96 tomographs (second column from the left in Figures 6 and 5a respectively) represent resistivity changes caused by roughly equal salt water volumes in the soil. A comparison of these two figures shows that the top two images in each column (those closest to the tank) are shaped differently. Simulations presented in Ramirez et al (1995) show that the anomalies are deformed, particularly those close to the tank probably due to the high resistivity contrast between soil and metal. The remaining six images in each of the figures suggest that the resistivity ratios observed in 1996 are closer to 1.0 (no change relative to baseline) than those observed in 1994. This means that the 1994 changes in soil resistivity are somewhat larger in magnitude than the changes in 1996. We believe that the smaller changes observed in 1996 are due to the remnants of the salt water plume created during the 1994 and 1995 tests. This remnant plume: 1) reduced the resistivity contrast between the salt water solution released and the pore water in the soil and 2) increased the moisture content of the soil when the 1996 baseline surveys were collected. The combined effects of higher moisture content and higher pore fluid conductivity would have reduced the resistivity of the soil when the baseline surveys were collected, thereby decreasing the change in resistivity caused by the 1996 salt water release.

The shapes of the anomalies observed in the two experiments are also somewhat different. There are several possible causes for the differences. 1) The images in Figure 6 (1994) are somewhat smoother than those in Figures 5a and 5b (1996). Higher quality data (better signal to noise ratio) was collected in 1996 because an instrument with much wider dynamic range was used. Also, as indicated by LaBrecque et al., 1996, the objective function minimized by the inversion algorithm consist of two parts: one part seeks to minimize model roughness and the other part seeks to minimize the misfit between the measured and calculated data. As the noise of the data increases, the resulting images are smoother because the part of the objective function which minimizes model roughness becomes more important. 2) We speculate that the shape and extent of the flowpaths in 1996 changed relative to 1994 because the moisture content of the partially saturated soil in 1996 was higher and the matric potential was

lower than in 1994. Similar comments can be made regarding the tomographs of 7/31/94 and 6/03/96 (rightmost column of tomographs in Figures 5a and 6.

2.2 Two dimensional resistivity change tomographs in the presence of an active leak:

In this section, we consider the scenario where a tank is actively leaking when the first ERT surveys are made. In this case, a radioactive nitrate plume is penetrating the partially saturated soil surrounding the tank. Then, the active leak point starts releasing water at a higher flow rate due to the start of a sluicing operation into the region. In this scenario, the moisture content and fluid conductivity of the soil during the baseline surveys are higher than what would be observed in the preceding scenario, because now the salt water plume has much less time to drain. Thus, the changes caused by the increased leak flow rate may be smaller than those observed with a remnant nitrate plume.

Figure 7 presents two-dimensional tomographs showing the resistivity changes after the flow rate was increased from about 720 liters/day to about 1060 liters/day. The location of the release point remains the same. These resistivity ratios were calculated relative to the surveys of 6/03/96 after about 3600 liters had been spilled. The spill volumes presented are the difference between the total volume released for each date and the volume released as of 6/03/96. Also, the color scale used is different from that shown in Figures 5 and 6 because the changes in resistivity are smaller in this case. Time and leaked volume increase from left to right on the figure.

The images for June 4 and 5 (1996) at depths of 6.1 to 8.1m show detectable but small electrical conductivity increases directly below the release point close to the "path for vertical migration". Once again, the changes observed increase in magnitude as time and spilled volume increase. From Figures 7 and 5b we see that the shape and magnitude of the anomalies are roughly the same for the 6/06/96 tomographs (changes relative to the baseline of 6/03/96, collected after the flow rate was increased during the 1996 spill) in Figure 7 and the 6/03/96 tomographs in Figure 5/29 (changes relative to the baseline of 5/29/96, collected prior to the start of the 1996 spill). Each of these tomograph sets show changes after roughly the same volume of water has been spilled. Note that the anomaly shapes and magnitudes are similar. This suggests that increasing the flow rate did not change the water flow path in any significant way. In a tank farm setting, we may observe similar results when the baseline ERT surveys are collected during an active leak and when the baseline surveys sample soil by a leak which occurred in the past. We believe that this observation needs to be corroborated in a tank farm because the infiltration test used to simulate tank farm conditions was probably conducted on a much shorter time scale than a leak from a real tank that may have been leaking for months or years.

A comparison of Figure 5a and 5b (changes relative to the baseline of 5/29/96, collected prior to the start of the 1996 spill), Figure 6 (changes relative to the baseline of 6/23/94, collected prior to the start of the 1994 spill) and Figure 7 (changes relative to the baseline of 6/03/96, collected after 3600 liters had been spilled had been released during the 1996 spill) suggests the following

observations: 1) The largest resistivity changes observed developed during the first spill in 1994 (Figure 6) where the changes are calculated relative to pristine conditions. This expected result is due to the fact that the pre-spill soil probably had the lowest soil moisture and pore fluid electrical conductivity. When the first spill occurred in 1994, the resulting increases in moisture content and fluid conductivity caused the largest reductions in resistivity relative to the baseline surveys. 2) The resistivity changes caused by increased flow rate (Figure 7) of an active leak are roughly equivalent to the resistivity changes observed when a new plume invades a soil region containing a pre-existing plume (Figure 6). 3) In a tank farm environment, it appears possible to detect new plumes which develop over pre-existing plumes. This conclusion needs to be corroborated in a tank environment because the ionic strength of real tank fluids is significantly higher than that of the test salt water solution.

2.3 Three dimensional resistivity tomographs used without the benefit of pre-spill data:

One question which may be posed regarding the use of ERT for leak monitoring is whether it is possible to detect leaks without the benefit of pre-spill baseline surveys. It is known that individual tanks at Hanford have released contaminant plumes in years past. If these plumes change the resistivity of the soil in a detectable way, and these resistivity changes remain imprinted in the soil years after the leak became inactive, it may be possible to detect these plumes without the benefit of pre-spill data. These plumes may remain detectable over a significant period of time because the invaded soil has a higher moisture content and a higher pore fluid conductivity than the surrounding soil. All other conditions being equal, soils with a higher moisture content and pore fluid conductivity will have a lower resistivity than the surrounding soil.

One strategy that may be used to identify pre-exiting plumes is to look for regions of relatively low electrical resistivity under the tank. We note that regions of low resistivity can be due to natural causes such as changes in mineralogy (e.g. increases in clay content) and natural fluctuations in moisture content. Thus, low resistivity soil regions may be caused by remnant contaminant plumes as well as by normal soil heterogeneity. If this strategy is used to identify possible plumes, it will be necessary to have access to independent data (e.g. core samples, neutron well logs, gamma ray logs) in order to determine the root cause of the low resistivity region.

The results shown in this report and in Ramirez et al., (1995) show that plumes larger than several hundred liters change the soil in a detectable way when pre-spill data is available for comparison. The next question that needs to be evaluated is whether the leak-induced changes will remain detectable long after the spill event finished. In order to provide a partial answer to this question, we compared the resistivity measured before the first spill started in 1994 (6/94) to the resistivity measured before the start of the 1996 spill (5/96-6/96). During this period of time, three separate spills were conducted and a total of about 10750 liters were released. The last of the three spill tests ended in May of 1995. This means that the 1996 baseline surveys were collected one year after the end of the last spill. Drainage of excess pore water should have occurred during this

period and the remaining salt water should move very slowly due to the effect of capillary forces.

Figure 8 shows the results of this data comparison. The tomographs show that in 1996 there are soil regions which have a lower resistivity than in 1994. Note that tomographs at 3.0 m depth and below show relatively large regions with resistivity ratios smaller than 1.0. We believe that these changes are due to the spills conducted in 1994 and 1995. Rain water infiltration can be ruled out as a cause for these anomalies because measurements conducted during significant rainfall events have shown that rain induced resistivity changes are basically undetectable at depths of 1.5 m and below. Thus, the results in Figure 8 suggest that the remnant of the 1994 and 1995 plumes remained detectable for at least one year. Summarizing, we propose that leaks of the order of several thousand liters cause easily detectable changes in soil resistivity, and these changes remain imprinted in the soil for a period of at least a year.

The next question is whether it is possible to map contaminant plumes when ERT pre-spill measurements are unavailable, that is, resistivity change tomographs are no longer possible and only tomographs of absolute resistivity are available. This is a scenario considered likely for many tanks at Hanford, because the spills occurred years before any ERT surveys were performed. This situation requires that a "plume imprint" caused by previous spills be somehow recognized in the absolute resistivity structure of the soil surrounding a tank. It is necessary to model the tank resistivity structure explicitly in order to correctly map the resistivity structure around a tank because of the significant effect that the tank's metal has on current flow in the soil. A fully three dimensional tomography inverse algorithm is necessary in this case. Using the field test results obtained over a 2 year period and a 3D inverse code, we generated 3D tomographs of resistivity structure surrounding the tank. With these tomographs we then evaluated whether the plume imprint is recognizable in resistivity tomographs.

Figure 9 shows three dimensional ERT tomographs generated from data collected during the leak. In this case, the data are used to calculate the resistivity changes within a block underneath the tank (instead of as a series of two dimensional slices such as those shown in Figure 2 using only data from electrodes located at 1.5 m, 6.1 and 10.7 m depth). The 3D reconstruction shown in Figure 9 is 21.3 m wide, 21.3 m. long and 10.7 m. tall and is the reconstructed volume bounded by the electrode arrays in the sixteen holes around the tank. The 3D images may provide a better view of the changes caused by the leak because: a) the flow regime is truly three-dimensional, so there is no need to assume that the resistivity extends to infinity in the third dimension, b) there is no need for interpolation between adjacent 2D slices, and, c) the effect of the metallic barrier is explicitly accounted for in the 3D images but not in the 2D images. However, the 3D images takes much longer to calculate (5 hours per tomograph block) than the 2D images (5 minutes per tomograph plane).

The top two images in Figure 9 show three dimensional tomographs of resistivity. The tomographs show the resistivity structure before any salt water spills had affected the site (June 1994) and the resistivity structure obtained with data

collected in May of 1996, after three salt water spills had affected the soil below the tank. These spills were conducted from each of the three release point shown in Figures 2 and 9. A total of 10700 liters were released between the time the two data surveys were taken and the last spill concluded in May of 1995, one year before the 1996 data was taken. The top left hand tomograph shows that the soil under tank in 1994 was heterogeneous with a 0.75 order of magnitude contrast between the high and low resistivity regions. The top right tomograph shows that the soil in 1996 has a somewhat larger resistivity contrast of about 1.0 order of magnitude.

The top right tomograph in Figure 9 is an example of the resistivity information that would likely be available when the first ERT survey is collected a year (or more) after the spill occurred. One strategy that could work in this situation is to look for the regions of low resistivity as possible indicators of the plume. The top row of elements in each of the top two tomographs shows a region of low resistivity that is caused by the presence of the tank metal, so these elements need to be disregarded. The low resistivity region (blue in color) observed in the NE quadrant of the tomograph between depths of 7 and 10.5 m is a good candidate indicator of a plume. If we had the benefit of the 1994 data for comparison (top left tomograph in Figure 9), we could clearly see that the low resistivity anomaly observed in 1996 is not present in 1994; other changes could be seen as well, as illustrated by the percent resistivity difference image in Figure 9. Without the 1994 data, we would first have to decide whether the low resistivity zone: 1)is a credible indicator of a plume, or, 2)is caused by natural soil heterogeneity such as changes in soil mineralogy. If independent data (such as core logs or geophysical well logs) are available and indicate that the less resistive region is not likely caused by natural heterogeneity, then we may decide to consider this anomaly as an indicator of the presence of a plume.

The next question we address is how well correlated are the leak volume estimated without baseline data and the leak volume estimated when baseline data are available. A comparison of the top right and bottom tomographs in Figure 9 can be used to illustrate the answer to this question. For this discussion, we will assume that resistivity changes larger than 10% are reliable indicators of the plume location. The region of largest percent difference in the bottom tomograph roughly coincides with the low resistivity anomaly in the top right tomograph. The bottom tomograph shows that a large fraction of the volume below the tank shows percent resistivity decreases between -20% and -100 %. The top right tomograph shows that the volume occupied by the low resistivity anomaly is a small fraction of the total volume. This means that relying on low resistivity anomalies as plume indicators will likely result in a significant underestimation of the total plume volume.

An important cause of this discrepancy is the confounding effect that natural heterogeneity has on our ability to define the margins of the low resistivity anomaly. We would expect that this effect gets worse with increasing natural soil heterogeneity. For example, the low resistivity anomaly (top right tomograph in Figure 9) could be caused by slight increases in the clay content of the sand in this part of the sand layer. We can only rule out this possibility because we have

available the 1994 tomograph which does not show a region of low resistivity in the same area; thus, we know that the anomaly was due to a change that developed over time and not due to spatial changes in clay content (which remain invariant over time).

The work reported by Ramirez et al. 1995, indicated that the 3D images take much longer to calculate (5 -6 days hours per tomograph block) than the 2D images (20 minutes per tomograph plane). Since then, improvements in the 3D algorithm, coupled with increases in CPU processing speed have reduced the amount of time needed for the 3D images to about 5 hours (all others aspects of the problem remaining the same). This means that, if the 3D technique were to be used for leak detection during sluicing operations, tomographs could be available several hours after data collection ended.

3.0 Summary And Conclusions:

This document provides a summary of a field experiment performed under a 15 m diameter steel tank mockup located at the Hanford Reservation, Washington. The purpose of the test described here was to more closely represent the conditions which may exist around tanks surrounded by contaminant plumes and determine whether it is possible to: 1) use resistive changes to image a contaminant plume as it developed in soil under a tank already contaminated by previous leakage, 2) use resistivity changes to image a contaminant plume when an active leak is present and current activities cause the leak flow rate to increase, and 3) use absolute resistivity tomographs to map a contaminant plume beneath a tank without the benefit of background (pre-spill) data. A brine release experiment was conducted from 5/29/96 to 6/10/96 at the leak test facility. About 11000 liters of saline solution were released along a portion of the tank's edge. The release rate was varied from about 30 liters/hour to about 44 liters/hour, depending on the ERT data being taken.

The 1996 field test is, in many ways, a replica of a test conducted in 1994 and reported in Ramirez et al 1995. A key difference between the 1996 and 1994 tests is that the 1994 test was conducted in a pristine soil environment, whereas the 1996 test was conducted in a soil contaminated by three separate spills. Resistivity change tomographs from the 1996 test show that the 1994 changes in soil resistivity are somewhat larger than the changes in 1996; we believe that smaller changes observed in 1996 are due to the remnant salt water plume created during the 1994 and 1995 tests. The 1996 resistivity change tomographs also show that the changes caused by increasing the flow rate of an active leak are roughly equivalent to the resistivity changes observed when a new plume invades a soil region countering a pre-existing plume. In a tank farm environment, it appears possible to detect new plumes which develop over pre-existing plumes. This conclusion needs to be corroborated in a tank environment because the ionic strength of real tank fluids is significantly higher than that of the test salt water solution.

Resistivity change tomographs based on data collected in 1994 and in 1996 suggest that leak-induced changes are easily detectable and remain imprinted in the soil for a period of at least a year. Absolute three dimensional tomographs of

resistivity were used in an attempt to map contaminant plumes when ERT pre-spill measurements are unavailable. Visual inspection of the 3D tomographs suggest that low resistivity anomalies associated with the plume may be visible. However, such anomalies could also be due to natural heterogeneity of the soil and independent data would be needed to correctly interpret the source of the anomalies. The 3D results also suggest that using low resistivity anomalies as plume indicators will likely result in a significant underestimation of the total plume volume. An important cause of this discrepancy is the confounding effect that natural heterogeneity has on our ability to define the margins of the low resistivity anomaly.

4.0 Acknowledgments:

The work of many people was needed to ensure the success of this project. D. Iwatate and S. Narbutovskih, Westinghouse Hanford Co., coordinated site activities, helped plan the tests, and provided general field support. Mark Sweeney of Westinghouse Hanford Co. also provided field assistance and supporting equipment.

This work was performed under the Environmental Programs Directorate at LLNL. It was funded by the Characterization, Monitoring and Sensors Tech. Program, Office of Technology Development, U.S. Department of Energy (DOE). The Tank Focus Area provided funds to operate and maintain the experimental test site at Hanford.

5.0 References:

Cruse, J., D. Iwatate, K. Tollefson, R. Treat, T. Trenkler, and R. Lewis, 1995, Functions and Requirements for Hanford Single-Shell Tank Leakage Detection and Monitoring, WHC-SD-WM-FRD-021, Westinghouse Hanford Co, Richland, WA.

LaBrecque, D. J., M. Miletto, W. Daily, A. Ramirez, and E. Owen, 1996, The effects of Noise on Occam's Inversion of Resistivity Tomography Data, *Geophysics*,, vol. 61, no. 2,.pp. 538-548.

LaBrecque, D., and G. Morelli,1996, 3-D Electrical Resistivtiy Tomography for Environmetal Monitoring, Proceedings of the Symposium on the Application of Geophysics to Engineering and Environmental Problems, Keystone, CO, April 28-May 1, 1996; sponsored by the Environmental and Engineering Geophysical Society.

Narbutovskih, S., W. Daily, A. Ramirez, T. Halter, and M. Sweeney, Electrical Resistivity Tomography at the Hanford Site, *Proc. Symposium on the Application of Geophysiscs to Engineering and Environmental Problems*, Keystone, April 28 - May 2, 1996.

Ramirez, A., W. Daily, A. Binley, D. LaBrecque and D. Roelant, 1995, Detection of Leaks in Underground Storage Tanks Using Electrical Resistance Methods, UCRL-JC-122180, Lawrence Livermore National Laboratory, accepted for publication in *J. Engineering and Environmental Geophysics*.

Reidel, S. P., K. A. Lindsey, and K. R. Fecht, 1992, Field Trip Guide to the Hanford Site, WHC-MR-0391, Westighouse Hanford Corp., Richland, WA.

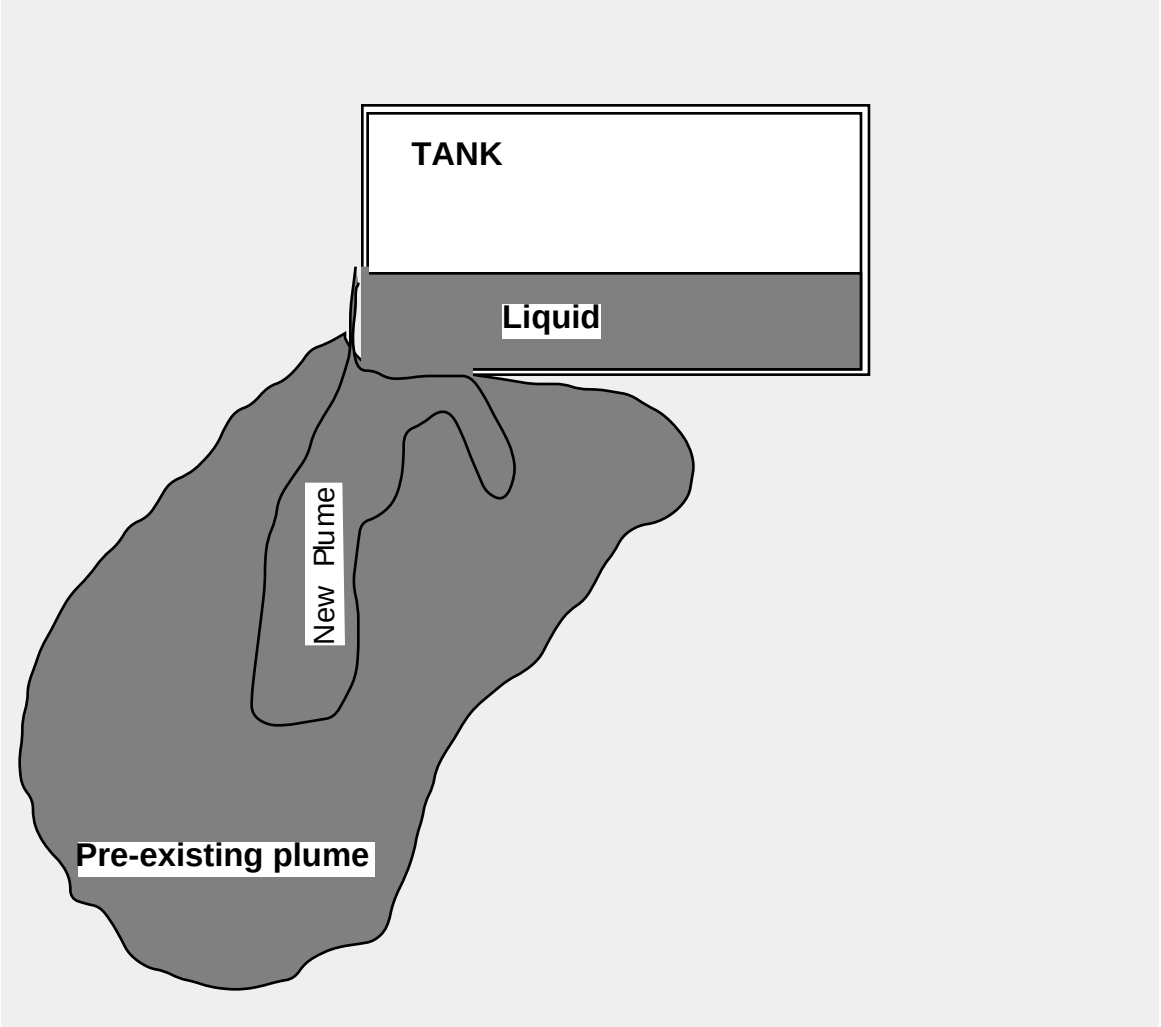

Figure 1 shows the tank leakage scenario physically modeled by the test described here.

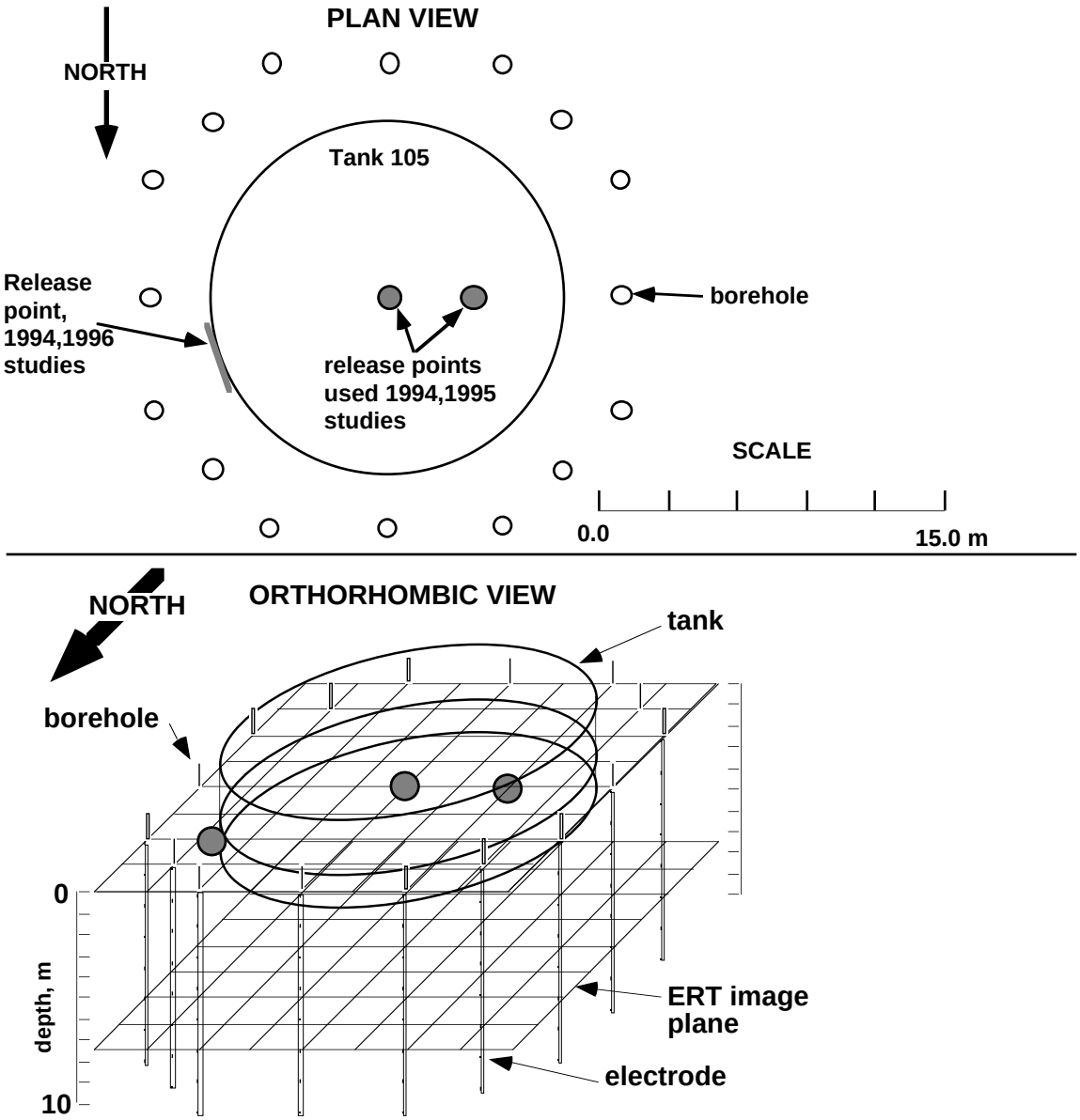

Figure 2. Schematic of experimental set up for leak detection. A 15 m diameter steel tank, the lower 2 meters of which is buried, contains several built-in spill points. Note that the release point on the East side of the tanks is the one used for this study. The other two release points and the one to the East were used in 1994 and 1995 to conduct other leak experiments. Sixteen boreholes, with eight electrodes in each, surround the tank.

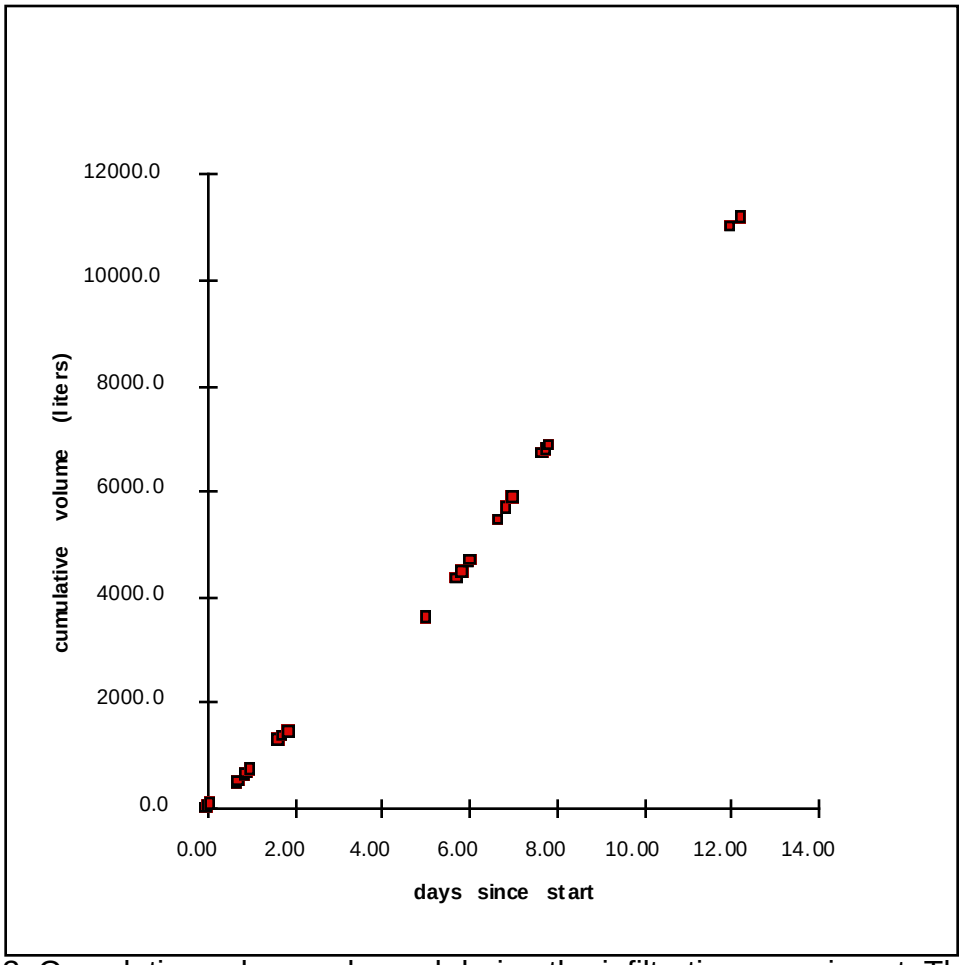

Figure 3. Cumulative volume released during the infiltration experiment. The flow rate (as indicated by the slope of each line segment) started at about 30 liters/hour for the first 5 days and then increased to about 44 liters/hour. Day 0.0 equals 5/29/96 at approximately 3:30 PM.

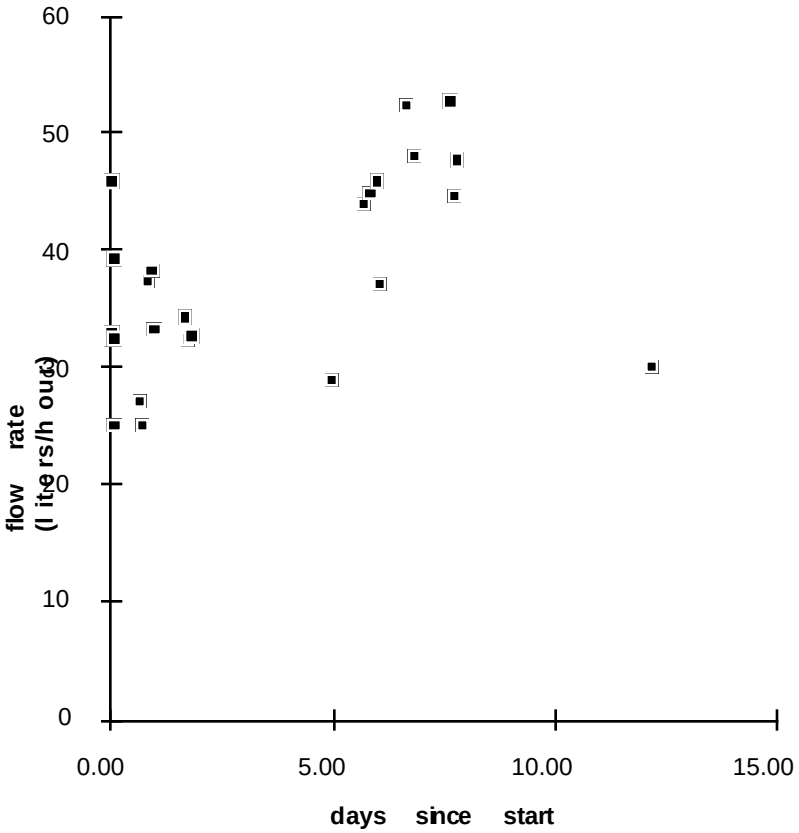

Figure 4. Instantaneous flow rate during the infiltration experiment. The flow rate averaged about 30 liters /hour for the first 5 days and then increased to an average of about 44 liters/hour for the remainder of the test. Day 0.0 equals 5/29/96 at approximately 3:30 PM.

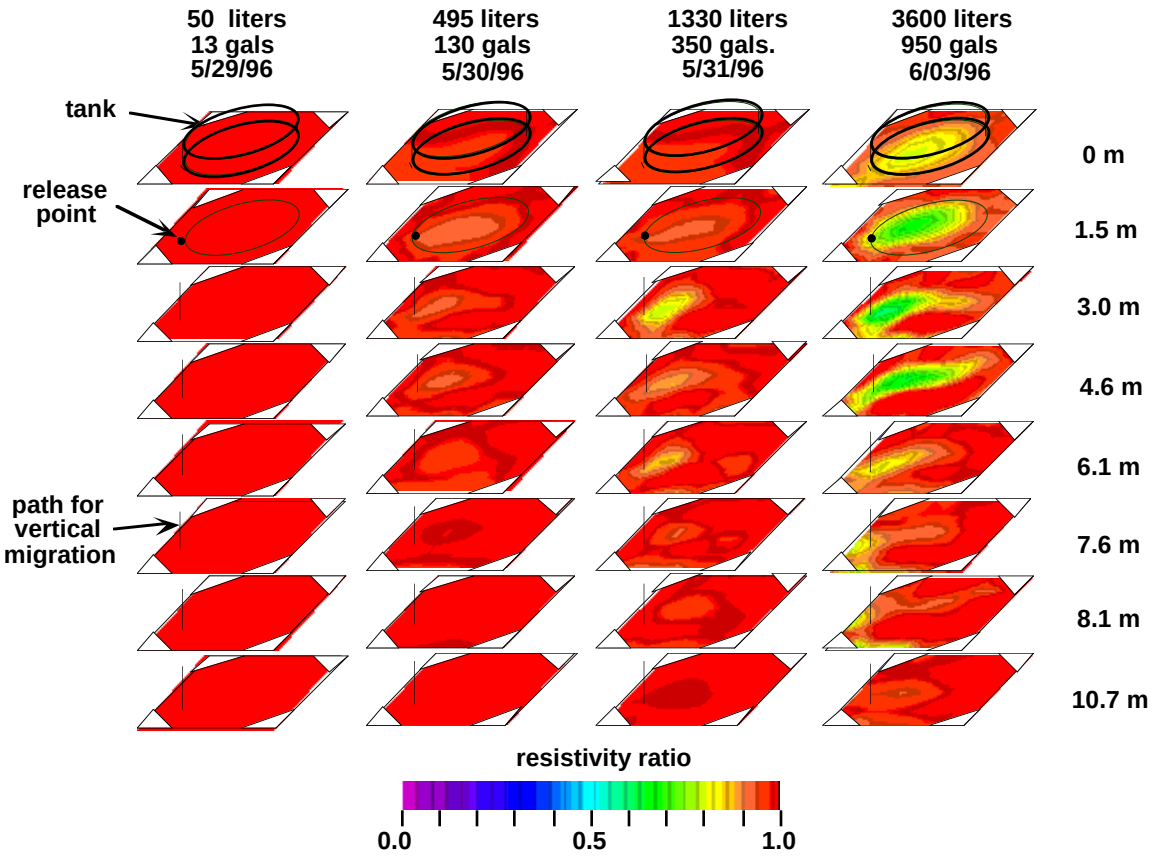

Figure 5a presents a series of two-dimensional resistivity change tomographs which show how the electrical resistivity of the soil decreased during a salt water release experiment conducted in 1996. These resistivity ratios were calculated relative to the baseline surveys of 5/29/96. Note that these baseline surveys were collected after about 10,700 liters had been spilled in 1994 and 1995. Red indicates which portions of the images remain unchanged (ratio = 1.0). Increasingly yellow and green tones indicate which portions of the image show electrical resistivity decreases associated with the leak. A vertical dotted line shows the trajectory the brine would follow if it moved straight down.

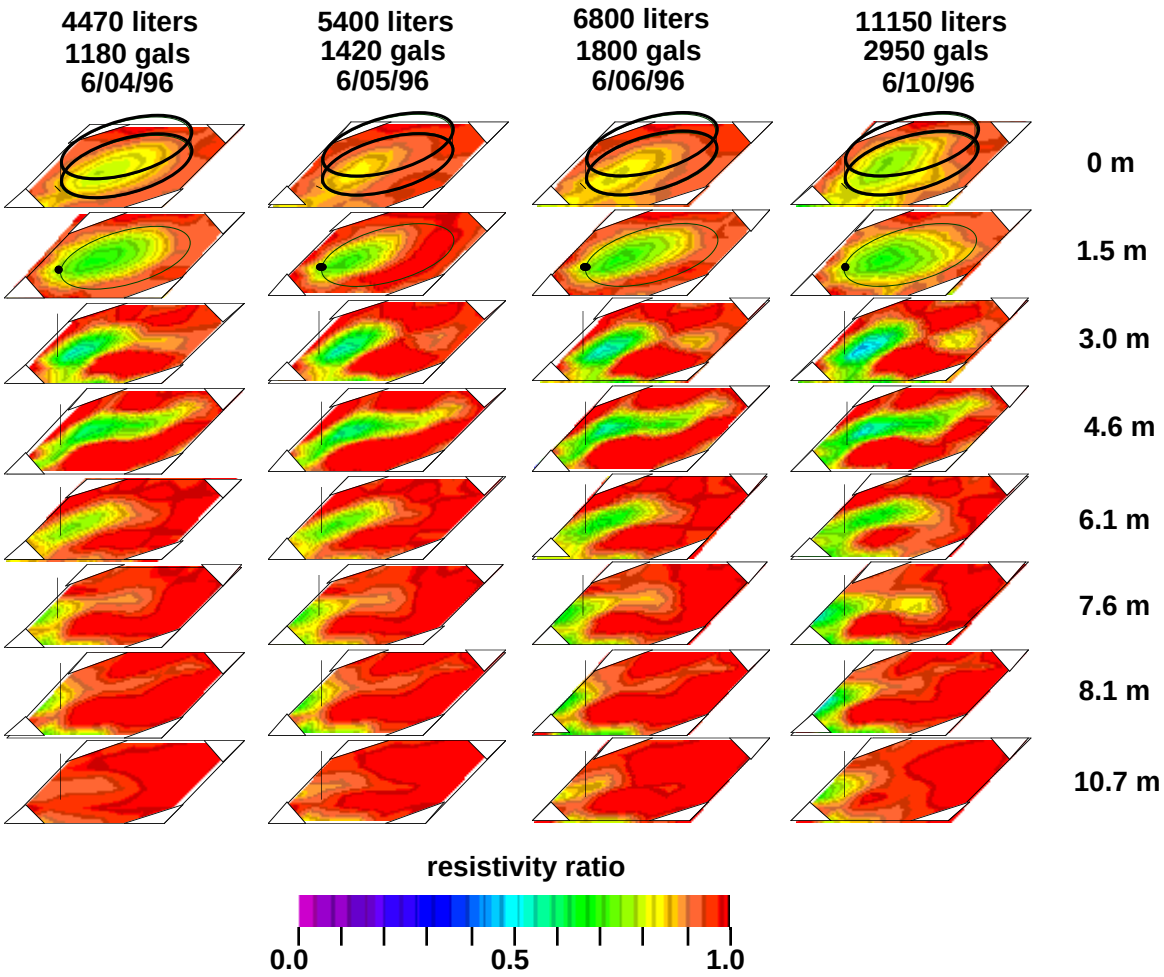

Figure 5b shows the continuation of the time sequence of tomographs which began in Figure 5a.

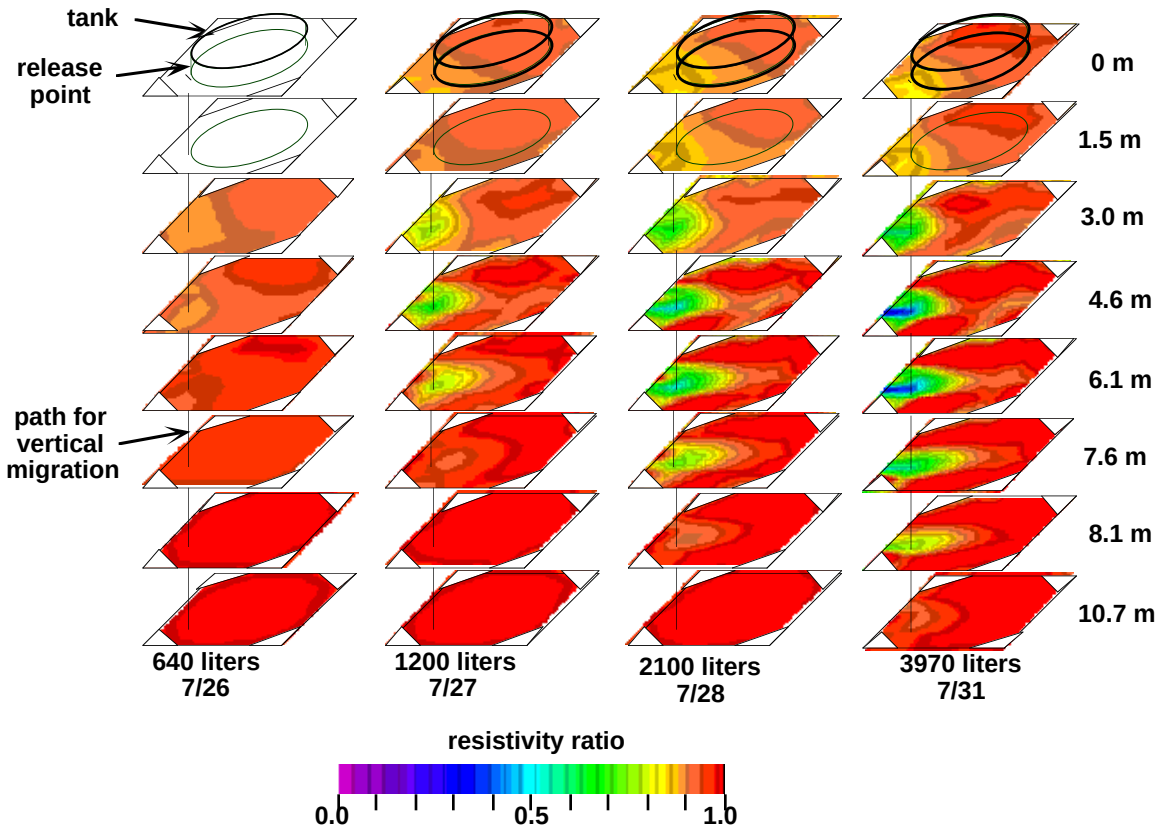

Figure 6 shows a series of two-dimensional resistivity change tomographs which show how the electrical resistivity of the soil decreased during the salt water release experiment conducted in 1994. These resistivity ratios were calculated relative to the baseline surveys of 6/23/94. Note that these baseline surveys were collected before the soil under the tank was invaded by salt water tracer. The image scale used is identical to that used for Figure 5 a and b for ease of comparison.

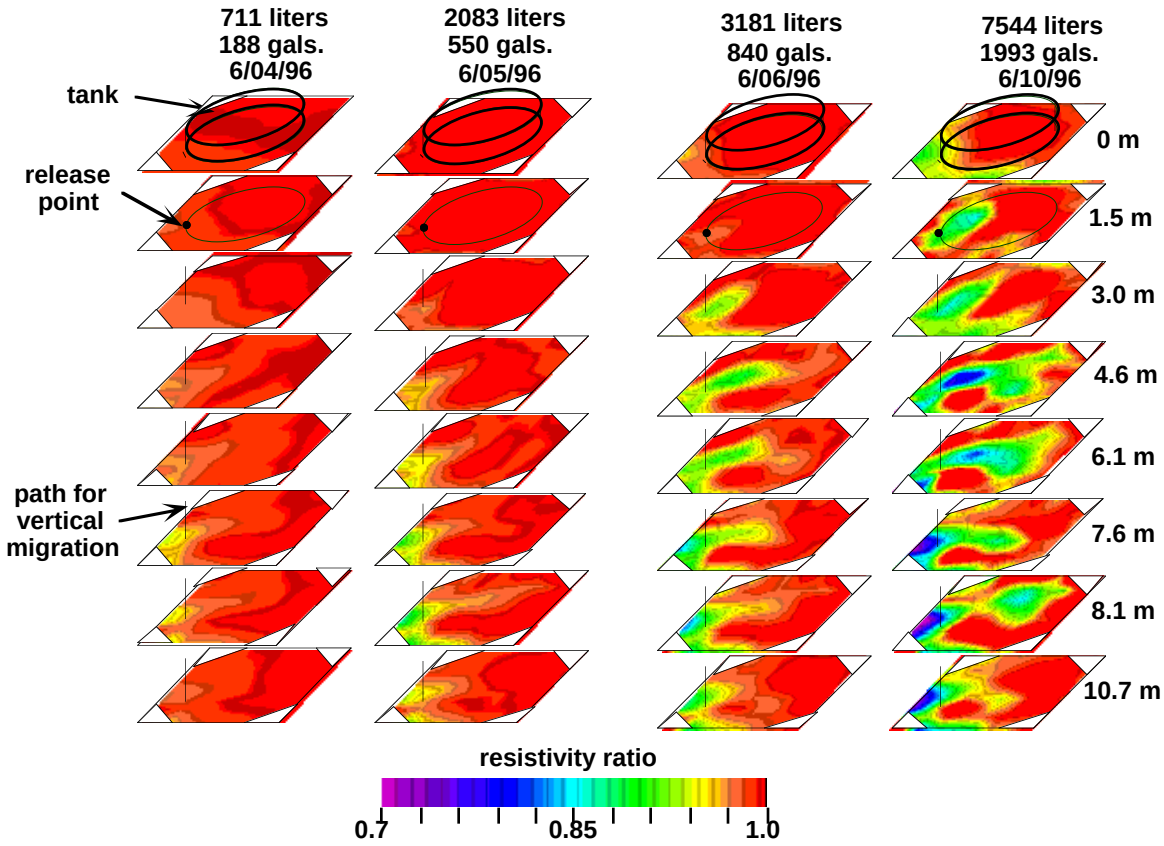

Figure 7 presents a series of two-dimensional resistivity change tomographs which show how the electrical resistivity of the soil decreased during the side release experiment. These resistivity ratios were calculated relative to the surveys of 6/03/96. Note that these surveys were collected after about 3700 liters had already been spilled in 1996. The spill volumes presented are the difference between the total volume released for each date and the volume released as of 6/03/96. The color scale used is different from that shown in Figures 5 and 6 because the changes in resistivity are smaller in this case. Red indicates which portions of the images remain unchanged (ratio = 1.0). Increasingly yellow and green tones indicate electrical resistivity decreases associated with the leak.

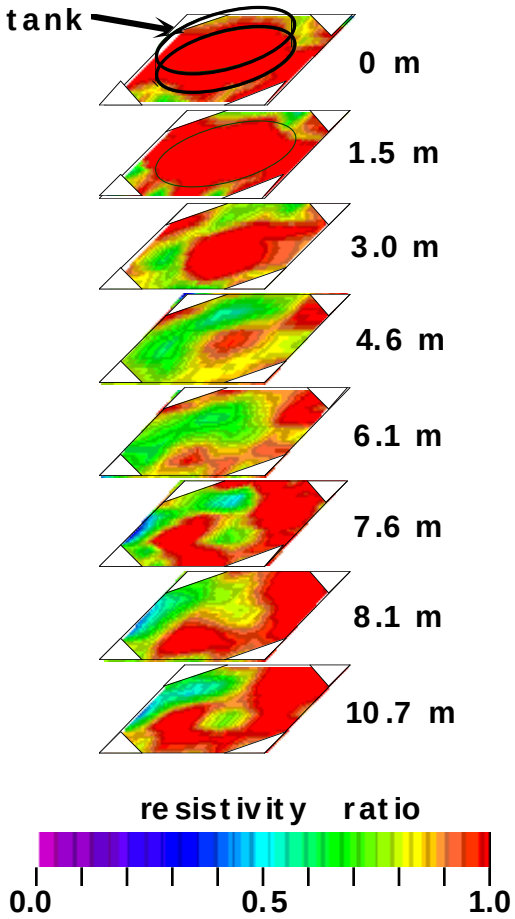

Figure 8 shows the resistivity changes calculated when the 1996 pre-spill data is compared to the 1994 baseline. The resistivity ratios show that the 1996 resistivities remain lower than the 1994 resistivities. This suggests that remnants of the salt water plumes released in 1994 and 1995 are still detectable in 1996.

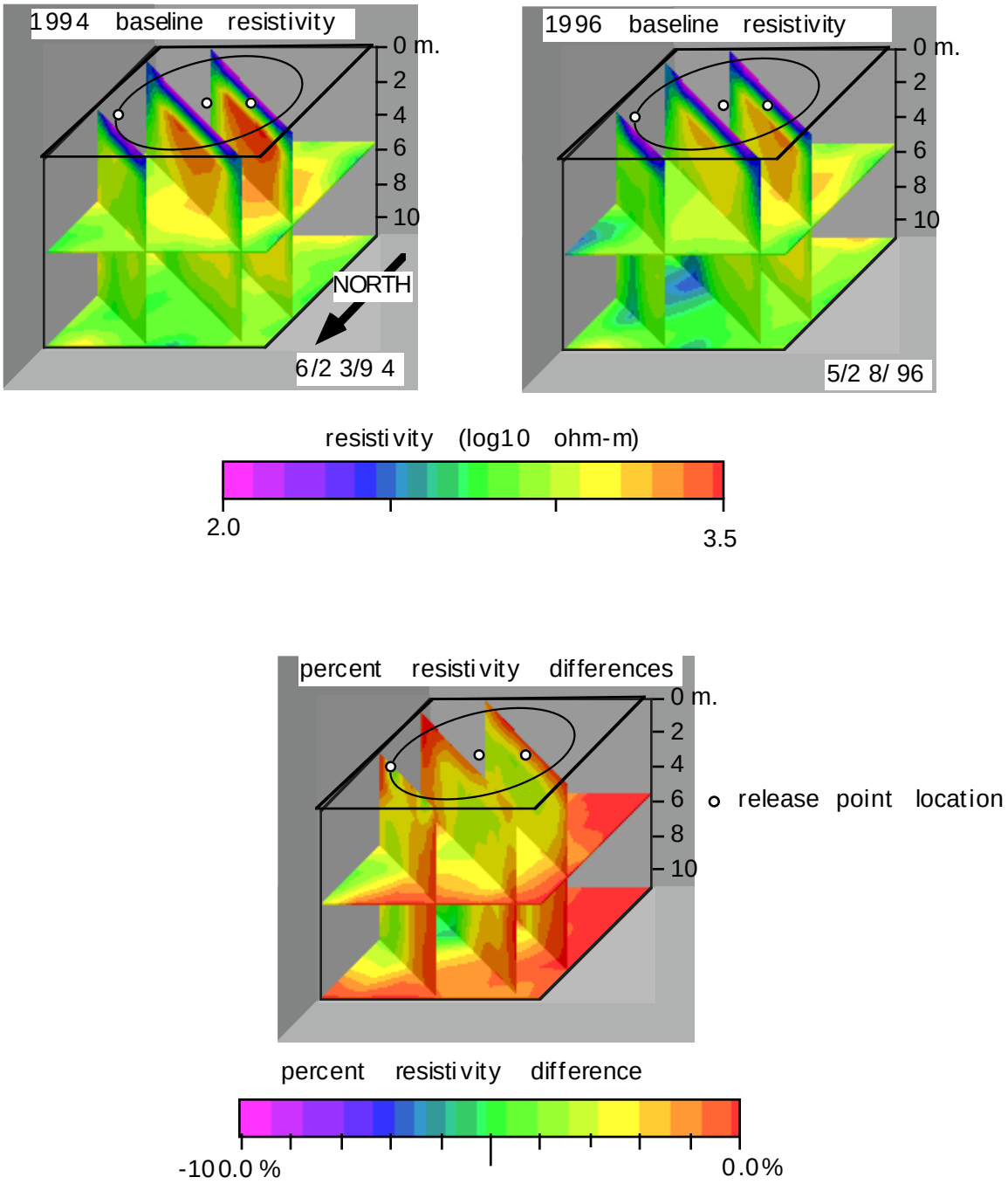

Figure 9 shows three dimensional tomographs of resistivities. Slices through the block are shown and the remaining block volume is transparent in order to see inside the volume. The upper two tomographs are the baseline resistivity structures obtained before the beginning of the 1994 and 1996 spills. The upper two tomographs are displayed using a logarithmic scale. The bottom figure shows the cumulative percent resistivity change between the 1994 and 1996 baseline resistivity tomographs; this image is displayed using a linear scale. The resistivity changes were caused by salt water releases from each of the release points shown. The total volume spilled during this time was about 10700 liters.